Regular and chaotic phase synchronization of coupled circle maps

Grigory V. Osipov

Institute of Physics, University Potsdam 10, Am Neuen Palais, D-14415, Potsdam, Germany
and Department of Radiophysics, Nizhny Novgorod University, 23, Gagarin Avenue, Nizhny Novgorod 603600, Russia

Jürgen Kurths

Institute of Physics, University Potsdam 10, Am Neuen Palais, D-14415, Potsdam, Germany

We study the effects of regular and chaotic phase synchronization in ensembles of coupled nonidentical circle maps (CMs) and find phase-locking regions for both types of synchronization. We show that synchronization of chaotic CMs is crucially influenced by the three quantities: (i) rotation number difference, (ii) variance of the phase evolution, and (iii)relative duration of intervals of phase increase respect decrease. In the case of regular CMs, only variance and rotation number difference are important. It is demonstrated that with increase of noncoherence of phase evolutionsin the regular and chaotic regime, the regions of the main (1:1) synchronization are usually decreased. We present a chaotic synchronization in the systems of coupled non-identical circle maps where phase entrainment occurs and it is not accompanied by bifurcations of the chaotic set. For ensembles (chains) of coupled CMs with linear and random distributions of the individual frequencies soft and hard transitions to global synchronization are found.

I. INTRODUCTION

Synchronization of oscillations is one of the fundamental nonlinear phenomena in biology, physics, chemistry, communication, and many other branches of science and engineering [1]. Synchronization of periodic systems studied since Huygens is understood now sufficiently well. The appearance of periodic synchronization is manifested through a frequency entrainment that implies phase locking, i.e., the existence of bounded shifts between the phases of interacting elements. Recently, the phenomenon of phase locking has been also observed in systems of coupled chaotic oscillators [2]. That chaotic phase synchronization (CPS) has been studied in the cases (i) of an external force acting on a chaotic system [3,4], (ii) of interaction between two chaotic systems [5] and in ensembles of (iii) globally [6] and (iv) locally [7] coupled chaotic oscillators. First examined for paradigmatic dynamical model systems: Rössler and Lorenz oscillators, the CPS has been observed in many real systems, in particular electrically coupled neurons [8,9], ecological systems [10], human cardiorespiratory system [11], and in magnetoencephalograms [12] and electroencephalograms [13]. All these systems are time continuous. Many systems in the nature and technology and their corresponding mathematical models are discrete in time, because of that it is also necessary to consider analogous synchronization phenomena in ensembles of coupled time-discrete elements.

In this paper we study conditions for an onset of regular and chaotic phase synchronization in small (two elements) and large (chains) ensembles of coupled nonidentical circle maps (CMs). For networks of coupled maps different problems of synchronization, pattern formation, and spatiotemporal chaos have been extensively investigated [14–16]. But in most previous studies identical coupled elements were analyzed. It is evident that for networks of coupled identical elements the investigation of CPS has no sense because the individual frequencies of the uncoupled elements already coincide. We consider here coupled nonidentical elements, i.e., a more realistic case that usually arises in nature where subsystems are never identical. In contrast to other time-discrete dynamical systems, the CMs are such objects for which the phase variables yet exist that allows to use the criteria of synchronization similar to criteria used by the detection of CPS in time-continuous systems. Synchronization in ensembles of complex systems has found important practical applications in electronics, radioengeneering or communications, in particular, in networks of digital phase-locked loops (DPLL) [17–21]. Systems of coupled CMs can be used as a rather simple but a paradigmatic model to investigate processes of mutual synchronization in coupled relaxation systems. In this case, the phase variable can be interpreted as an onset of a new impulse [1,22]. The system under consideration belongs to the broad class of ''pulse-coupled'' systems arising in many branches of science and technology; e.g., pulse-coupled systems have been investigated as models of neural networks [23], cardiac pacemaker cells [24], or in communication [25]. It is important to note that systems with the phase variable as a dynamical variable but time continuous are subject of great interest in connection with different applications in biological [26] and chemical [27] systems, Josephson junction arrays [28], or laser arrays [29].

The paper is organized as follows. In Sec. II we shortly describe the behavior of the CMs under study, and introduce three main characteristics of the phase evolution of a single CM. A model of chains of coupled CMs and criteria of synchronization in these chains are discussed in Sec. III. In Sec. IV we present our numerical results of regular and chaotic phase synchronization in two-element systems. Section V is devoted to synchronization in chains of coupled CMs with linear and random distribution of the natural frequencies. The results are summarized in Sec. VI.
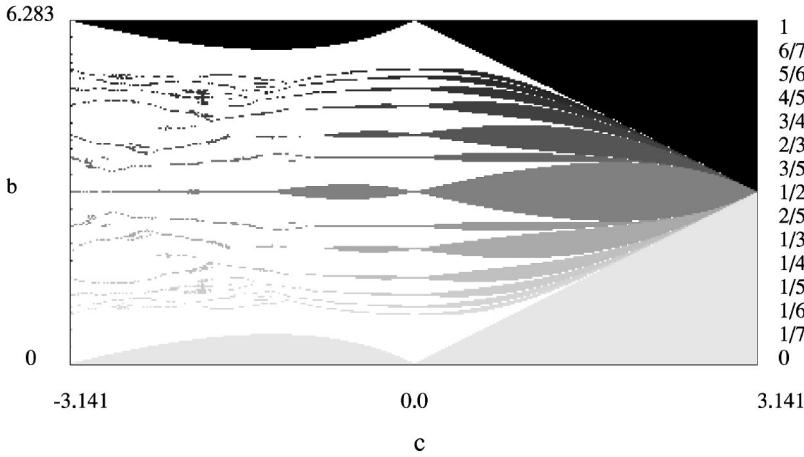
FIG. 1. Distribution of rotation numbers of the circle map (1). Several regions where the rotation numbers are rational ($\rho=p/q$) are presented. From the bottom to the top the different gray level regions are ordered as shown on the right side. Between these regions there exist (but not presented) relatively small regions with other rational rotation numbers.

II. DYNAMICS OF INDIVIDUAL CIRCLE MAP

We consider the circle map as the basic element of the ensembles studied here,

$$x^{k+1}=b+x^k-F(x^k). \tag{1}$$

This map relates the phase variable x^k at adjacent times $k=1,2,\ldots$; $b\in[0;2\pi]$ is a positive parameter that can be interpreted as frequency; $F(x)$ is a piecewise linear 2π-periodic function of the form $F(x)=cx/\pi$ defined in the interval $[-\pi,\pi]$, and c is the control parameter. System (1) is one of the basic models in nonlinear dynamics, and it has been studied in many mathematical (cf., Ref. [30]), physical (cf., Ref. [31]) and technical (in particular, in the theory digital phase-locked loops [20,32,33]) issues. Recently, for piece wise function $F(x)$ diffusive like phenomena have been observed in such a system [34]. Our choice of a piecewise linear function $F(x)$ is motivated not only by simplicity of consideration (see, for example, Refs. [21,34]) but also by the fact (see Case 3 below) that chaos is observed in the system for all $c<0$ and there is no stable periodic orbits for any $c<0$. Moreover, our numerical simulations show that the effects observed in this paper also exist for other functions $F(x)$, in particular, for $F(x)=c\sin(x)$.

First, we shortly recall basic properties of this circle map. It has for $b<|c|$ a unique fixed point $x_f=b\pi/c$ that is stable if $x_f\in[0;\pi]$ (Case 1 below) and unstable if $x_f\in[-\pi;0]$ (Case 3).

The dynamics of an individual CMs can be determined by the rotation number ρ, which in both types of dynamics (regular or chaotic) is defined as the average growth rate of the phase

$$\rho=\frac{1}{2\pi}\lim_{M\to\infty}\frac{x^M-x^1}{M}, \tag{2}$$

where M is the number of iterations.

There are three types of behavior of Eq. (1) [33,35]
(i) Case 1:

$$\left|1-\frac{c}{\pi}\right|<1. \tag{3}$$

Here the map derivative is less than one, i.e., it is locally contracting. In the interval $b<c$ the fixed point is stable and there occur three variants:

(a) For every value of b Eq. (1) has the only attractive set Ω. For a rational rotation number $\rho=p/q$ this set is an attracting periodic trajectory of period q; for an irrational rotation number the set Ω is a Cantor set on which Eq. (1) acts as a rotation.

(b) With b varying, the rotation number ρ depends continuously on b and does not decrease monotonously.

(c) For each $\rho=p/q$ there is a corresponding interval of b that is not reduced to a point. The dependence of ρ on b is shown for different values of c in Fig. 1. With increasing of c, the number and width of intervals of b, in which the rotation numbers are rational, are increased. Thus at relatively large values c even uncoupled CMs are synchronized. As we will show below, this property plays a decisive role for the synchronization in ensembles of coupled regular CMs.

(ii) Case 2:

$$\left|1-\frac{c}{\pi}\right|=1. \tag{4}$$

If $1-c/\pi=1$, then Eq. (1) becomes a continuous map of a circle rotating through b. In this case the dynamics of two coupled CMs have been considered in Ref. [18]. If $1-c/\pi=-1$, then Eq. (1) remains a continuous map of a circle.

(iii) Case 3:

$$\left|1-\frac{c}{\pi}\right|>1. \tag{5}$$

Here we are in a chaotic regime because the Lyapunov exponent $\lambda=\ln|1-(c/\pi)|$ is positive. Its nonwandering set consists of a finite number of intervals on which repelling periodic orbits are dense, and there is a finite number of repelling periodic orbits. For almost all values of the parameter b this set is a nontrivial attractor. The dependence of the rotation numbers on the individual frequency for small $|c|$ looks like the case of periodic motions (Fig. 1), i.e., there are a number of intervals with rational rotation numbers. If $-c$ increases, all these regions are firstly increase and then shrinking and consequently the rotation
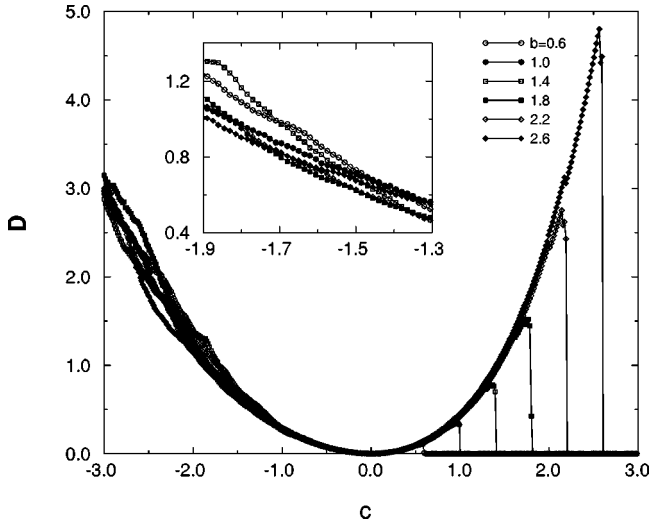
FIG. 2. The variance D of x^k (6) vs c for map (1) at different values of the frequency parameter b.

FIG. 3. Phase evolution at $b=0.6$ for different c for map (1).

numbers are irrational in an increasing part of the considered interval of b. As we will show below, this is manifested in different synchronization properties of regular and chaotic motions at relatively large c.

The parameter c defines the coherence properties of the motions. As a measure of the power of coherence, we use the variance D that can be defined for large k as

$$D = \langle (x^{k+1} - x^k - \langle x^{k+1} - x^k \rangle)^2 \rangle, \qquad (6)$$

$\langle . \rangle$ defines time averaging. So for $c=0$ (Case 2), the rotations are completely coherent and $D=0$. If $|c|$ grows, the noncoherence properties of rotation are increased. The dependence of D on the parameter c at different values of b shows rather different features (Fig. 2): for periodic motions it can be well fitted by the curve $D=0.42c^{2.5}$, but for chaotic motions by the quadratic curve $D=0.29c^2$. We explain this effect as follows. For regular rotations (Cases 1 and 2) the phase x^k only monotonously increases. For chaotic motions, however, we can distinguish two different types of phase evolution: In the first type x^k only monotonously increases. The second type is represented as an alternation of intervals, where the phase increases, with intervals, where the phase decreases. Both types of phase evolutions in the cases of regular ($c=0, 0.5$) and chaotic ($c=-0.5, -1.0, -1.5, -2.0,$ $-2.5, -3.0$) motions are presented in Fig. 3. For $b>0$ the mean duration of phase increase intervals is usually considerably larger than the mean duration of phase decrease intervals. Therefore, this type of motion looks like intermittency of relatively large intervals of phase increase and short intervals of phase decrease. It can be easily shown that the first type of the motion exists for $b<-c$. Both types of behavior can be characterized by the ratio of the number of iteration where the phase is increasing and where the phase is decreasing. Let us denote N_g the number of phase increase iterations and N_d the number of phase decrease iteration and look at the parameter $\gamma = N_d/N_g$. Then, we easily see that for $b<-c$, $\gamma=0$, but otherwise $\gamma \neq 0$ (Fig. 4).

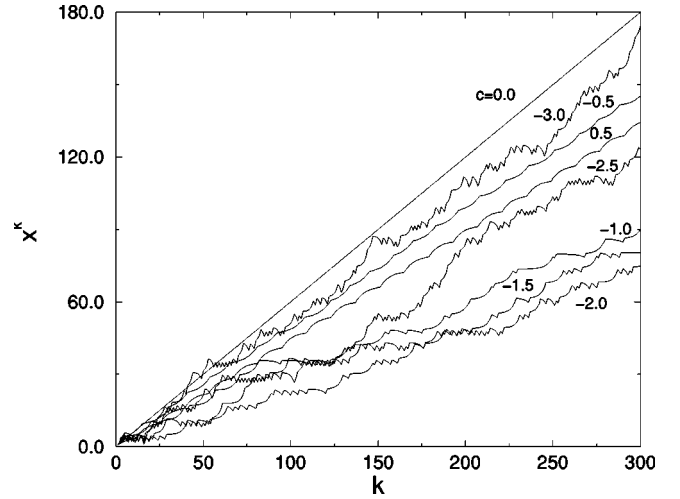We will show below that for the synchronization of chaotic CMs the three parameters: variance D, parameter γ, and difference of rotation numbers of interacting elements are crucial, whereas for regular CMs only the variance D and the difference of rotation numbers are important.

III. ENSEMBLES OF COUPLED CIRCLE MAPS AND CRITERIA OF SYNCHRONIZATION

As the main model we study a chain of nonidentical CMs that are locally coupled

$$x_n^{k+1} = b_n + x_n^k - F(x_n^k) + d[\sin(x_{n+1}^k - x_n^k) + \sin(x_{n-1}^k - x_n^k)]. \qquad (7)$$

Here $n=1,\ldots,N$ corresponds to the number of individual CMs and d is the coupling coefficient. The parameters b_n characterize the partial frequencies. We assume that the system is subjected to free-end boundary conditions: $x_0^k = x_1^k$ and
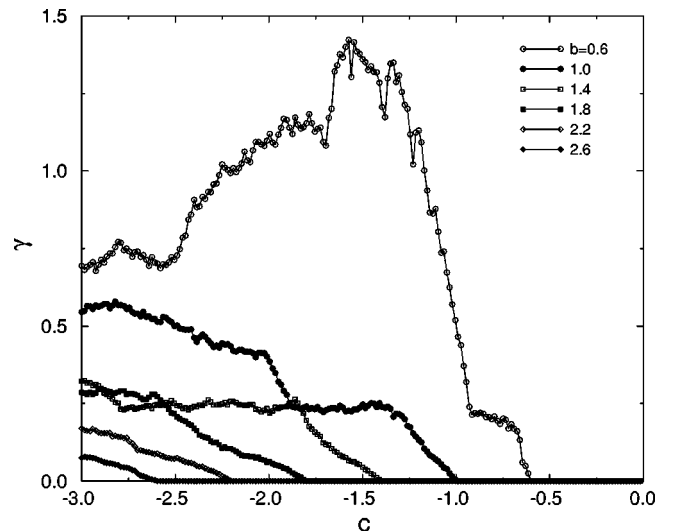

FIG. 4. Ratio of the duration of phase decrease intervals to the duration of phase increase intervals in dependence on c at different values of b.

$x_{N+1}^k = x_N^k$. System (7) can be regarded as a model of a multichannel chain of partial DPLL connected in parallel by phase-mismatching signals. To realize these connections in the chain in its simplest variant, it is necessary to compare the output signals of two neighboring DPLL generators with the help of a separate phase discriminator and then to apply the obtained phase-mismatching signal for the frequency control of both generators. Some similar one dimensional and two dimensional in space models of coupled identical CMs have been studied in Ref. [21].

We analyze the nonlinear coupling between partial elements in the form of *sinus* of phase differences also because such kind of coupling naturally arises in models of ensembles of weakly coupled time-continuous oscillators. Respectively, pattern formation and synchronization in networks of phase oscillators with coupling between nearest neighbors have been investigated in Ref. [36]. For populations of such periodic elements with different partial frequencies, the existence of global synchronization is observed, i.e., all elements of the population are synchronized, but also several clusters of synchronized rotators exist. In contrast to often used types of diffusive coupling like linear phase difference between neighbors,

$$d(x_{n+1}^k - x_n^k) + d(x_{n-1}^k - x_n^k), \tag{8}$$

or through the same nonlinear functions as individual functions for each element

$$d(F[x_{n+1}^k] - F[x_n^k]) + d(F[x_{n-1}^k] - F[x_n^k]), \tag{9}$$

the *sinus* type of coupling exhibits some special properties of the dynamics of populations of time discrete elements. It is important to emphasize that the *sinus* coupling (7) generates mutual synchronization already for a very small coupling d compared to the cases (8) and (9). To give one example for a two-element system at $c = 0.05$ and $b_1 = 0.1$, the critical value of $\Delta b = b_2 - b_1$ for which 1:1 synchronization can be achieved is $\Delta b = 0.01$ for Eqs. (8) and (9), whereas we get for the nonlinear coupling (7) synchronization in the large range $\Delta b \in [0:6]$ (see also Fig. 5).

Another speciality here is that all presented types of coupling can lead to a loss of synchronization when the coupling parameter d is increased (see also Ref. [37]). To show that we consider the system of two coherent ($c=0$) CMs coupled as in Eq. (7). By introducing a new variable $\theta^k = x_2^k - x_1^k$, the mutual dynamic of two CMs can be defined by the following *sinus* circle map:

$$\theta^{k+1} = \Delta b + \theta^k - 2d \sin \theta^k. \tag{10}$$

The fixed point $\theta^* = \arcsin(\Delta b / 2d)$ is stable for $d < 1$ and corresponds to a 1:1 regular synchronization in the original model (7) with constant in time phase difference θ^*. With increasing of parameter d, a period doubling cascade takes place that ends up in a chaotic behavior of the oscillatory type (i.e., θ^k is bounded). Note that the rotation numbers of the coupled CMs coincide here. But at some critical value d^*, the oscillatory chaotic attractor is changed into a rotationally chaotic one (i.e., θ^k is unbounded) that leads to the
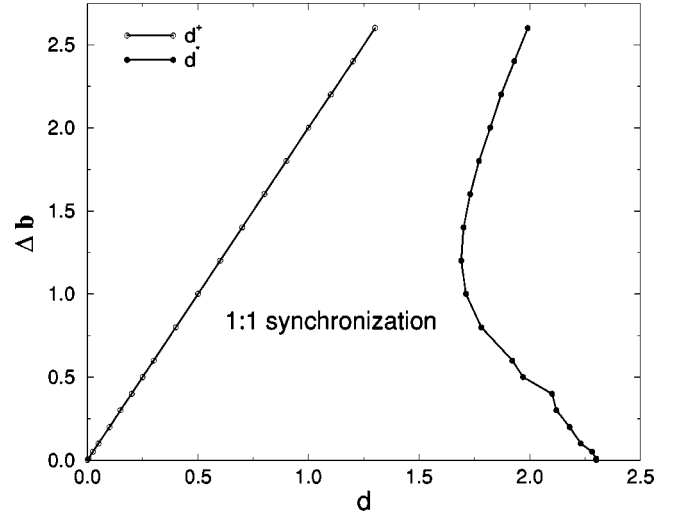

FIG. 5. Critical values of coupling d^+ and d^* corresponding (i) to the transition from nonsynchronous to synchronous motion (left curve) and (ii) to the transition from synchronous to nonsynchronous motion (right curve) in the model (13) vs frequency mismatch Δb. Between both curves there is the region of 1:1 synchronization.

loss of synchronization in the two-element model (7). This effect will be discussed in more detail in Sec. IV A. Also for the N-element system (7) in dependence on the number of elements and on the parameter c, there is a critical coupling value d^* corresponding to the transition from synchronous to nonsynchronous behavior. Note that a *desynchronization* bifurcation (see Ref. [37]) in which the increase of the coupling between elements in the coupled ensembles may destabilize the synchronous state are observed in many physical systems [38]. The phenomenon, called *short-wavelength bifurcation*, has been also seen in systems with phase variables, such as phase-locked loops or Josephson junctions [20,39].

We will use two criteria to test for $m_1 : m_2$ synchronization, where $m_{1,2}$ are integers. $m_1 : m_2$ phase synchronization of regular rotations as well as chaotic regimes between two CMs can be defined as phase entrainment or locking

$$|m_1 x_n^k - m_2 x_{n+1}^k| < \text{const}, \tag{11}$$

for all $k = 1, 2, \ldots$. A weaker criterion for the analysis of both types of synchronization in a chain of coupled CMs is based on their rotation numbers (2), i.e., we test for

$$m_1 \rho_n = m_2 \rho_{n+1}. \tag{12}$$

Because of its simplicity of calculation and convenience of presentation we often use in the following the criterion (12). By the study of synchronization effects in a chain of coupled CMs, the fulfillment of the conditions (11) and (12) for all $n = 1, \ldots, N-1$ means the existence of global synchronization. If these conditions are satisfied only for several neighboring elements, we have a regime of cluster synchronization.

IV. SYNCHRONIZATION OF TWO COUPLED CIRCLE MAPS

First, we investigate systems of two coupled CMs, described by the following equations:

$$
\begin{aligned}
x_1^{k+1} &= b_1 + x_1^k - F(x_1^k) + d \sin(x_2^k - x_1^k), \\
x_2^{k+1} &= b_2 + x_2^k - F(x_2^k) + d \sin(x_1^k - x_2^k).
\end{aligned}
\tag{13}
$$

As mentioned above, the effects of mutual regular and chaotic phase synchronization of two coupled systems can be characterized by the ratio of their individual rotation numbers $\rho_{1,2}$ or by the *winding* number: $w = \rho_2/\rho_1$ and by the evolution of the phase differences of CMs in time. It is important to emphasize that there is a remarkable difference in the synchronization for regular and chaotic CMs.

A. Regular synchronization

First, synchronization of two coupled CMs in regular regimes is studied.

1. Coherent case (c=0)

In the coherent case, i.e., $c=0$, the critical value of the coupling d^+ corresponding to the transition from nonsynchronous to 1:1 synchronous rotations can be easily found from the conditions of existence and stability of the fixed point for the *sinus* CMs (10): $d^+ = \Delta b/2$. Also the other critical value of coupling d^* corresponding to the transition from synchronous to nonsynchronous rotations can be found from the map (10) (cf., Refs. [40,41]). With increase of d the transition to chaos occurs via the period doubling scenario. This way we get chaos of an oscillatory type. The chaotic trajectory belongs always to the interval $[-\pi; \pi]$, i.e., the phase difference θ^k is bounded. In spite, that the rotation in our model (13) is chaotic, both criteria (11) and (12) are satisfied and 1:1 synchronization still exists. At some critical value of d^*, the chaotic regime becomes rotational, i.e., the phase difference θ^k unrestrictedly increases. This transition from oscillatory to rotational behavior of the phase difference is accompanied with a change in the geometry of the chaotic set. A sudden change in the type of the chaotic set occurs via *an interior crises* [42]; at this transition the 1:1 synchronization in the model (13) is violated. In Fig. 5 the dependences of the critical values d^+ and d^* on the frequency mismatch Δb are presented. As we will show below, these both values d^+ and d^* can be usually regarded as the lower and the upper estimates of the boundaries of the 1:1 synchronization region for both regular and chaotic rotations.

2. Noncoherent case (c≠0)

Now we analyze the synchronization properties of the regular CMs at different values of the coherence parameter c. As one can see from Fig. 1 for fixed values b_1 and b_2 with increasing parameter c, the individual rotation numbers ρ_1 and ρ_2, and therefore, the winding number w can be varied. Hence, we will study the two different cases of frequency distribution. We choose the individual frequencies $b_{1,2}$ in

such a way that for all considered values of c, the rotation numbers of the uncoupled CMs are (i) identical or (ii) can be different. The structure of the synchronization regions, their number and transitions from one synchronous region to another one can become very rich now. The dependence of w on the coupling parameter d for both cases [Figs. 6(a) and 6(b)] demonstrates clearly the existence of a lot of phase-locking regions; the number and width of them are increasing with increasing of c. So for $c=0$ only the 1:1 synchronization region [Figs. 6(a) and 6(b)] exists. For large enough values of c, synchronization between coupled CMs occurs not only as 1:1 synchronization but also as general $m_1:m_2$ synchronization (i.e., $m_1, m_2 \neq 1$). This $m_1:m_2$ synchronization is typical for coupled relaxation periodic oscillators for which the motions are noncoherent. For instance, in the system of two coupled strongly nonlinear van der Pol oscillators the synchronization occurs firstly as $m_1:m_2$ synchronization and only for larger coupling as 1:1 synchronization. As we can see from Fig. 2 with increasing c, the variance D increases too, and as a result of that the region of 1:1 self-synchronization becomes smaller for the first case of frequency parameters [Fig. 6(a)]. If c is larger than some critical value c^*, the 1:1 synchronization is impossible because of very strong noncoherence of the rotations. In the second case the size of the 1:1 synchronization region can surprisingly increase or decrease. In dependence on the values b_1 and b_2 the rotation number difference $\Delta\rho$ can increase or decrease. Therefore, at fixed parameters b_1 and b_2 with increase of c, synchronization can occur sometimes at smaller coupling and sometimes at larger coupling [Fig. 6(b)].

B. Chaotic synchronization

In systems of two coupled chaotic CMs some different synchronization properties are observed. We have performed numerical simulations for fixed $b_1 = 0.6$ and different values of b_2 (Fig. 7). Usually there exists only the region of 1:1 synchronization. Only in rather small intervals of c, regions of $m_1:m_2$ synchronization can occur. It should be noted that in all our presented experiments only $m_1:1$ synchronization with different $m_1 = 2,3,4,\ldots$ are observed. Figure 7 indicates that the geometrical structure and the sizes of the synchronization regions strongly depend on c which, as discussed above, defines the complexity of the behavior of the uncoupled elements. It is obvious that the processes of rotation locking in the system of coupled elements cannot be exactly predicted from the properties of motion of the uncoupled elements. As it was demonstrated in the regular case, even a weak coupling can already lead to a strong change in the mutual dynamics. But some common rules of appearance and disappearance of synchronization can be obtained and explained by knowing properties of the behavior of single elements. Considering the effect of c on the synchronization properties, we can roughly distinguish three intervals of c:

(i) small $-c$ where only a monotonously increase of the phases is possible in the interacting elements; in our experiments it was the interval $D_1: c \in [-b_1 = -0.6, 0]$;

(ii) large $-c$ for which the variance D is very large (see Fig. 2) and due to a high noncoherence of the motions, syn-
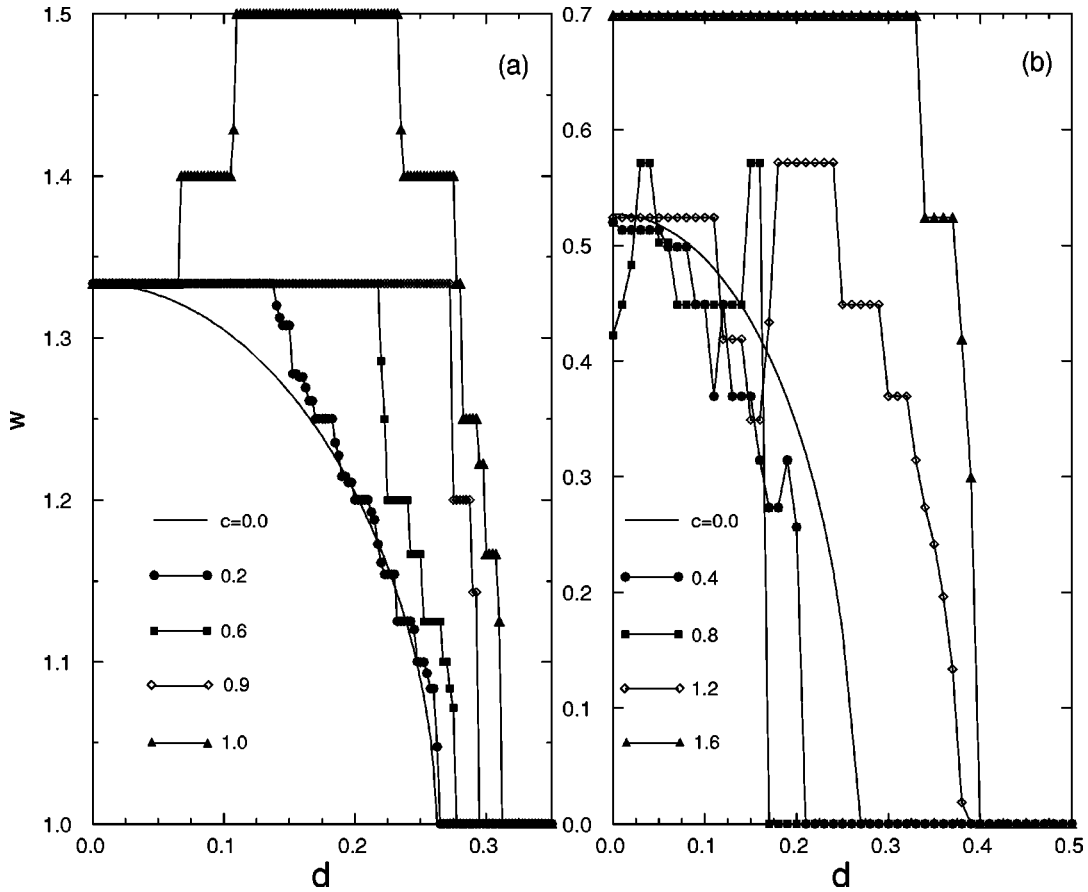
FIG. 6. The winding number w vs the coupling coefficient d at different c and $b_1 = \pi/2$, $b_2 = 2\pi/3$ (a), respectively, $b_1 = 4\pi/7$, $b_2 = 17\pi/23$ (b).

chronization cannot be achieved; in our simulation it was the interval $D_3 : c < -2.25$, and

(iii) intermediate c that do not belong to the two previously defined intervals; this is the interval $D_2 : c \in [-2.25; -0.6]$.

For each of these intervals we analyze influence of the three parameters on synchronization discussed in Sec. II, i.e., the variance D, the parameter γ characterizing the relative duration of intervals of phase increase, and phase decrease and the rotation number difference $\Delta\rho = \rho_2 - \rho_1$.

1. Small and large noncoherence

In the interval D_1 the difference of rotation numbers $\Delta\rho$ plays the crucial role in the synchronization. As in the case of regular coherent CMs (Sec. IV A 1), the critical value of coupling d^+, at which the transition to 1:1 synchronization occurs, depends on the value of the rotation number difference $\Delta\rho$. At larger values $\Delta\rho$ a larger value of coupling is needed to achieve synchronization. The sizes of the synchronization regions become smaller with increase of c. This happens due to increase of noncoherent properties of rotation. At chosen values b_1 and b_2 in the interval D_3 synchronization is in general impossible due to the highly noncoherent properties of rotations. For instance, at $c = -2.5$ and $b_1 = 0.6$ respectively $b_1 = 2.6$ we find that imperfect phase synchronization [43] (i.e., seldomly occurring phase slips are possible)

exists at the very small frequency mismatch $\Delta b = 0.0001$. Therefore, a very small frequency mismatch and as a result of that a very small rotation number difference does not always guarantee the occurrence of synchronization. The complexity, specifically noncoherence, of the behavior quantified by the variance of rotations D can be crucial. The existence of time intervals with a strongly different phase growth rate makes the processes of locking of rotations impossible.

2. Intermediate noncoherence

A quite different situation is observed in the interval D_2. For relatively small [(Figs. 7(a) and 7(b)] as well as large [(Figs. 7(h)–7(j)] frequency mismatches the main influence on synchronization is exerted by the rotation numbers difference $\Delta\rho$ and the variance D. But for intermediate values of Δb [(Figs. 7(c)–7(g)] initially synchronization is not achieved with an increase of c, for any values of coupling. For further increase of c, synchronization can appear again. The existence of such "islands" of synchronization can be qualitatively explained as follows. As it was mentioned above for chaotic rotations, two types of phase increase are possible: monotonous increase or alternation of intervals of phase increase and phase decrease. The transition to the second type of rotation occurs at $-c > b$. So for the first element with $b_1 = 0.6$ this critical value is equal to -0.6. Figure 4 indicates that γ (the ratio of the duration of the phase
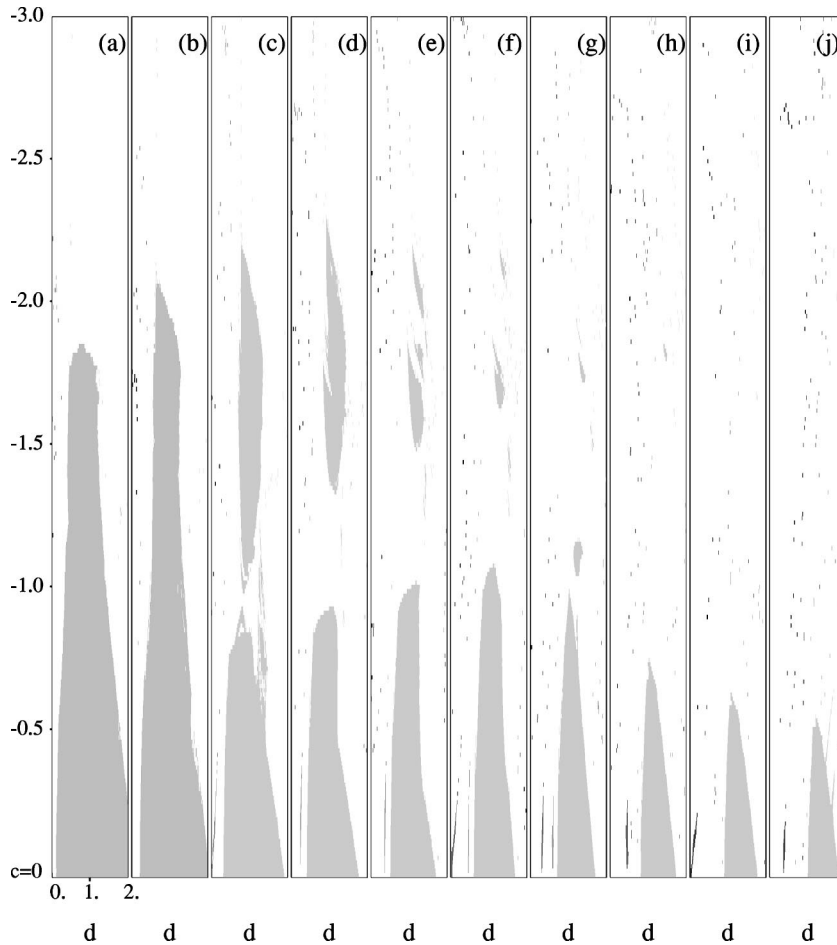
FIG. 7. Regions of chaotic phase synchronization for $b_1 = 0.6$ and different values of b_2: 0.8 (a), 1.0 (b), 1.2 (c), 1.4 (d), 1.6 (e), 1.8 (f), 2.0 (g), 2.2 (h), 2.4 (i) , 2.6 (j). The main gray regions correspond to 1:1 synchronization. In columns (c)–(j) for relatively small $-c$ small regions of 2:1 (c)–(g), 3:1 (f)–(h) and 4:1 (i),(j) synchronization are presented. They are visible as small stripes in the left bottom areas.

decrease intervals to the duration of the phase increase intervals for the first element) becomes strongly increasing at $c \approx -1$. If in the second element the phase is still monotonously increasing, then time intervals, where the phases rotate in opposite direction, are existing for coupled elements. This makes the phase entrainment rather difficult and usually phase synchronization does not exist [44]. If with increase of c in the second element phase decrease intervals appear, rotations in both elements becomes more similar, i.e., in both elements the phases can grow and vanish, and a phase entrainment can happen. We assume that this mechanism leads to existence of "islands" of synchronization for several values of frequency mismatch [(Figs. 7(c)–7(g)], because these "islands" appear at such values of c that approximately correspond to the transition to the second type of rotations in the second CMs.

C. Synchronized hyperchaos

Next we use the Lyapunov exponents to describe the occurrence of regimes of chaotic phase synchronization. For system (13) the Lyapunov exponents are given by

$$\lambda_1 = \ln\left|1 - \frac{c}{\pi}\right|,$$

$$\lambda_2 = \lim_{M\to\infty} \frac{1}{M} \sum_{k=1}^{M} \ln\left|1 - \frac{c}{\pi} - 2d\cos(x_2^k - x_1^k)\right|. \quad (14)$$

Since the first Lyapunov exponent λ_1 is constant and positive for all values of d, we expect that only the sign of the second Lyapunov exponent λ_2 is important for the occurrence of CPS. If both Lyapunov exponents are positive, we have *a hyperchaotic regime* that determines usually a nonsynchronized regime. If with increase of coupling the second Lyapunov exponent becomes negative, we have a strong indication for the occurrence of phase synchronization. This situation takes place at the transitions to 1:1 synchronization for all simulations presented in Figs. 7 and 8. Such bifurcation is observed in CPS of time-continuous systems (e.g., see Ref. [5]). But this is not the only one scenario for the transition from nonsynchronous to synchronous behavior for which criteria (11) and (12) are satisfied. We illustrate this with plots of dependences of the winding number w and the second Lyapunov exponent λ_2 on the coupling coefficient d (Fig. 8) and phase diagrams for nonsynchronous [Figs. 9(a) and 9(b)] and synchronous [Fig. 9(c)] regimes. In the interval $d \in [0.285,0.32]$ the winding number is equal $w = 3/1$ that corresponds to 3:1 synchronization, but the second Lyapunov exponent remains positive $\lambda_2 \approx 0.05$, i.e., synchronized hyperchaos exists. Also there are intervals of d in which 2:1 and 1:1 hyperchaos synchronizations are observed. The transition to (or from) synchronized hyperchaos are accomplished with a change in the structure of the chaotic set (Fig. 9). In the case of nonsynchronous hyperchaos [Figs. 9(a) and 9(b)] the chaotic trajectory covers practically the whole
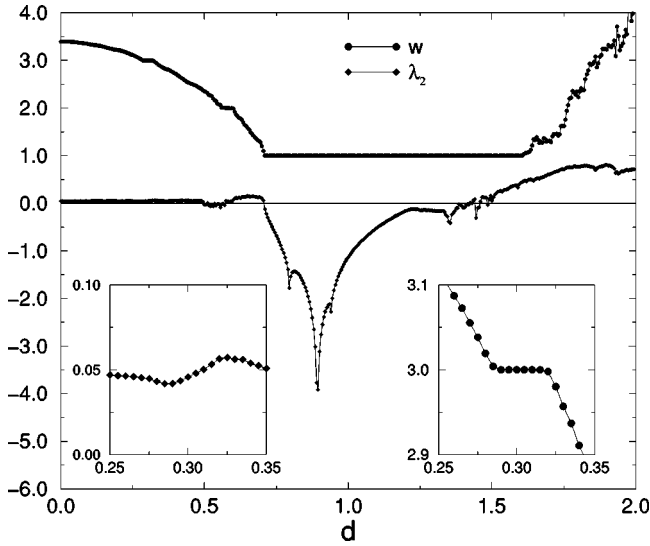
FIG. 8. The winding number w and the second Lyapunov exponent λ_2 vs the coupling coefficient d for $b_1=0.6$, $b_2=2.0$, and $c=-0.15$. Regions of 3:1, 2:1, and 1:1 synchronization are existing. Enlargements of the interval [0.25;0.35] are presented in the insets.

phase space: the square $[-\pi:\pi;-\pi:\pi]$ with different densities. When the value of coupling is close to the critical value corresponding to the transition to the synchronized hyperchaos, we observe localization of areas visited by chaotic trajectory. The appearance of more dense bands of motions can be clearly seen [Fig. 9(b)]. From the synchronization point of view the attendances of gaps between bands are corresponding to slips in the phase difference θ^k, i.e., jumps of 2π [45]. A decrease of the number of slips exhibits the tendency of the system to the perfect synchronization where no slips exist. At synchronized hyperchaos, the chaotic trajectory is placed only in relatively narrow bands in the phase space [Fig. 9(c)]. Like in the case of 1:1 synchronization of regular coherent CMs (see Sec. IV A 1), the transition to synchronous motions corresponds to the transition of the phase difference $\theta^k=x_2^k-3x_1^k$ from rotation to oscillation. Thus the transition from nonsynchronous to synchronous behavior in a two-element CMs system occurs through *interior crisis* [42] of the hyperchaotic set, i.e., for both regimes both Lyapunov exponents are positive.
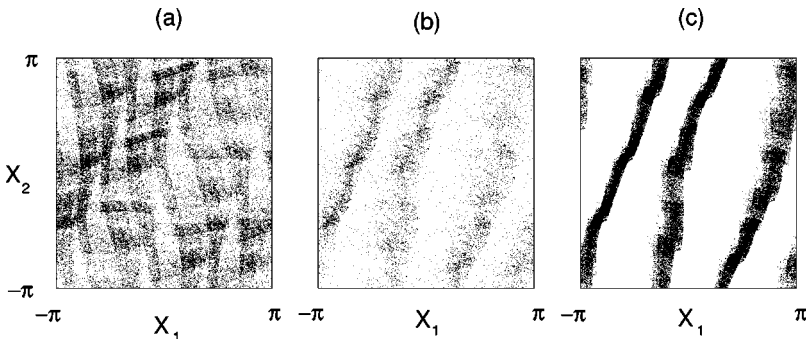
V. SYNCHRONIZATION AND CLUSTERING IN A CHAIN OF COUPLED CMS

To investigate synchronization in chains of N coupled CMs, we take first a linear increase of the individual frequencies:

$$b_n=b_1+\Delta b(n-1), \qquad n=1,\ldots,N, \qquad (15)$$

where Δb is the uniform frequency mismatch, and second a random distribution of the frequencies:

$$b_n=b_1+\Delta b\xi_n, \qquad n=1,\ldots,N, \qquad (16)$$

where $\Delta b=$const and ξ_n are uniformly distributed in the interval $[-0.5;0.5]$. In dependence on c we study three different cases which correspond to the three types of behavior of a single CMs: (i) coherent regular rotations ($c=0$), (ii) noncoherent regular rotations ($c>0$), and (iii) chaotic rotations ($c<0$).

A. Synchronization of coherent CMs

The system (7) for $c=0$ and a linear distribution of the partial frequencies b_n can be rewritten as

$$x_1^{k+1}=b_1+x_1^k+d\sin(\theta_1^k), \qquad (17)$$

$$\theta_n^{k+1}=\Delta b+\theta_n^k+d(\sin\theta_{n+1}^k-2\sin\theta_n^k+\sin\theta_{n-1}^k), \qquad (18)$$

$$n=1,\ldots,N-1,$$

with $\Delta b=b_{n+1}-b_n$, $\theta_n^k=x_{n+1}^k-x_n^k$ and the boundary conditions: $\theta_0^k=\theta_N^k=0$. The stable fixed point $\theta_n^{k+1}=\theta_n^k=\bar{\theta}_n$ for each $n=1,\ldots,N-1$ in system (18) corresponds to a regime of global synchronization in the chain. Then the system of equations for the stationary phase differences $\bar{\theta}_n$ can be written as

$$\Delta b+d(\sin\bar{\theta}_2-2\sin\bar{\theta}_1)=0,$$

$$\Delta b+d(\sin\bar{\theta}_{n+1}-2\sin\bar{\theta}_n+\sin\bar{\theta}_{n-1})=0, \qquad (19)$$

$$n=2,\ldots,N-2,$$

$$\Delta b+d(\sin\bar{\theta}_N-2\sin\bar{\theta}_{N-1})=0.$$

FIG. 9. Phase portraits of system (10) for $b_1=0.6$, $b_2=2.0$, $c=-0.15$ and different d within (c) ($d=0.3$) and outside (a) ($d=0.25$) and (b) ($d=0.275$) of the 3:1 synchronization region. In all three cases a hyperchaotic regime ($\lambda_1,\lambda_2>0$) exists.
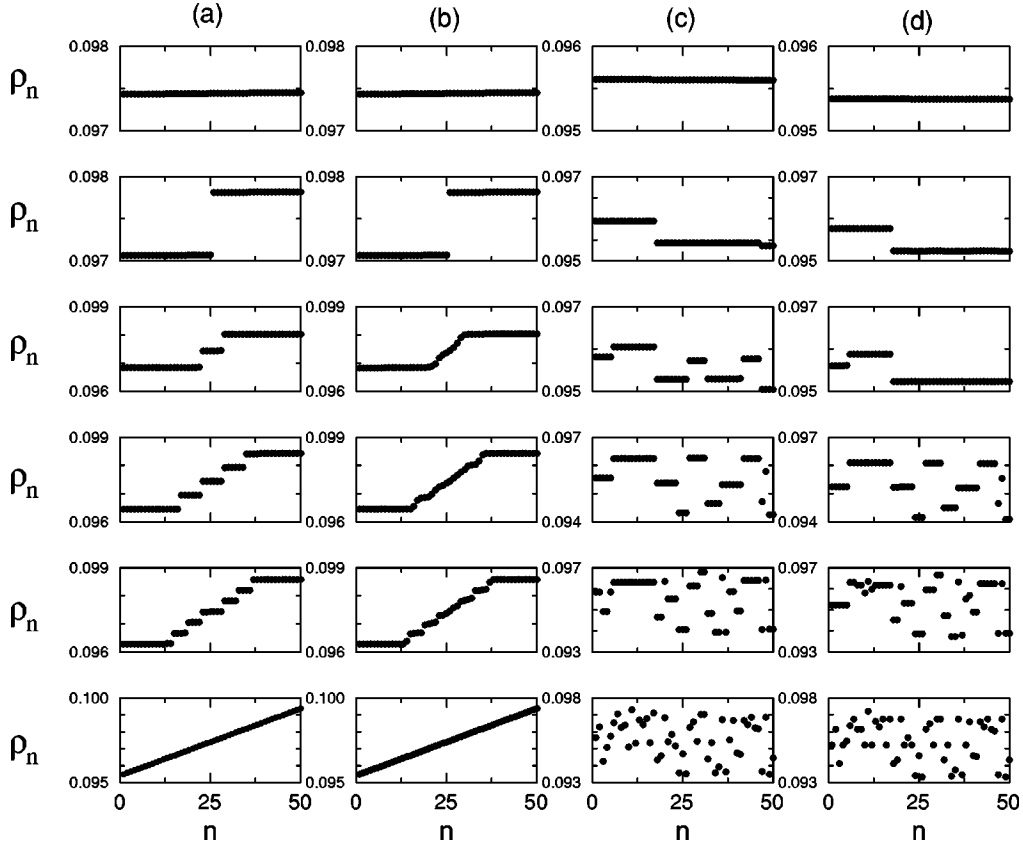
FIG. 10. Rotation number ρ_n distribution in the transition to global synchronization in coherent (a),(c) and noncoherent (b),(d) regimes. For a linear (a),(b) individual frequency distribution $b_n = b_1 + \Delta b(n-1)$ we take $b_1 = 0.6$, $\Delta b = 0.005$, $c = 0$ (a), $c = 0.000\,05$ (b) and coupling from bottom to top $d = 0, 0.03, 0.042, 0.08, 0.106, 0.158$. In the coherent case only clustered structures of synchronization are presented. For a random (c),(d) individual frequency distribution $b_n = b_1 + \Delta b \xi_n$ we take $b_1 = 0.6$, $\Delta b = 0.025$, $c = 0$ (c), $c = 0.05$ (d) and coupling from bottom to top $d = 0, 0.004, 0.008, 0.016, 0.02, 0.052$. ξ_n are uniformly distributed in the interval $[-0.5; 0.5]$.

As follows from Ref. [46], the distribution of $\bar{\theta}_n$ is

$$\sin \bar{\theta}_n = \frac{\Delta b}{2d}(Nn - n^2). \qquad (20)$$

It follows from Eq. (20) that the system (18) can have 2^{N-1} fixed points. As the frequency mismatch Δb is increased, the condition of the existence of fixed points

$$\left| \frac{\Delta b}{2d}(Nn - n^2) \right| < 1, \qquad (21)$$

is violated first for $n = N/2$ at even N, i.e., for the middle element in the chain. Thus, the condition for the existence of a fixed point in the N-element chain is given by the inequality

$$\left| \frac{\Delta b N^2}{2d} \right| < 1. \qquad (22)$$

This condition of global synchronization in system (7) coincides with the results of our numerical experiments. Then the rotation numbers for all elements are equal to the rotation number of the middle element $\rho_{N/2}$. However, with increasing of the frequency mismatch Δb a loss of global synchro-

nization takes place. For a long chain the two cluster synchronization occurs, i.e., the chain is divided into two clusters of equal sizes that consist of mutually synchronized CMs of different rotation numbers.

We have performed numerical simulations with a chain of 50 elements with linear [Eq. (15)] [Figs. 10(a) and 10(b)] and random distribution of individual frequencies [Eq. (16)] [Figs. 10(c) and 10(d)]. For each CMs we calculate the rotation number ρ_n. If all the rotation numbers are equal, we have global synchronization. If the rotation number are only equal for some groups of neighboring elements, cluster synchronization is formed. We have found that analogous to the self-synchronization in chains of periodic oscillators [47] and chains of chaotic phase coherent Rössler oscillators [7], mutual global synchronization in chains of coupled CMs can appear or vanish in two ways: soft and hard. The soft transition, i.e., transition without cluster formation, is characterized through a smooth locking of the rotation numbers and can be observed in the chains with very small frequency mismatch. But for the hard transition [Fig. 10(a)], transition through clusters, the appearance or disappearance of global synchronization is accompanied by the existence of cluster synchronization. This hard transition happens in long chains with relatively large frequency mismatch. As shown before, the loss of global synchronization leads to the appearance of
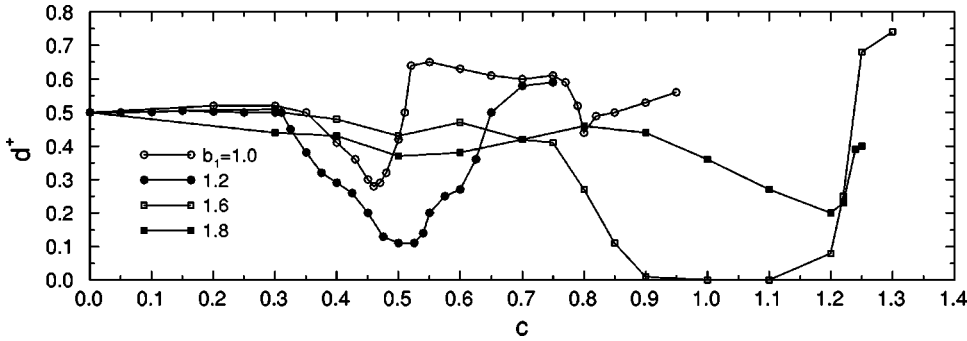
FIG. 11. Critical value of coupling d^+ corresponding to the transition to global synchronization vs c for different values b_1 and fixed $N=20$ and frequency mismatch $\Delta b = 0.01$.

two clusters of elements that rotate at the same rotation number. With further increase of the frequency mismatch the appearance of new clusters is possible. The values of rotation number for each cluster (except the edge ones) are close to those obtained by averaging the individual rotation numbers over all the elements forming the cluster. For the soft transition after the loss of global synchronization most elements of the chain (except, perhaps, the edge ones) rotate with different rotation numbers.

B. Effect of noncoherence of rotation on the regular synchronization

In this section we are going to elucidate how the increase of noncoherence ($c \neq 0$) influences the synchronization in chains. Our first finding is that the noncoherence can destroy the clusters of synchronization that are excited at coherent rotations. As our numerical experiments show for the linear distribution of individual frequencies b_n even for very weak noncoherence ($c=0.0001$), the transition to global synchronization is usually soft, and only the transition from a two-cluster structure to a one-cluster structure is hard [Fig. 10(b)]. The boundaries of clusters existing in the noncoherent case become first slightly smooth if the parameter c increases [Fig. 10(b)]. If the noncoherence increases ($c \approx 0.001$), all clusters except the edge ones are completely destroyed. Since there still exist a possibility of synchronization at relatively large c of uncoupled CMs, synchronization cluster structures can appear with further increase of c.

For randomly distributed frequencies b_n, synchronization clusters are more stable [Figs. 10(c) and 10(d)]. Small c does not practically change the number of clusters, the number of elements in the clusters and mean rotation numbers. With increase of noncoherence the transition to global synchronization through the appearance of clusters is still observed. Only the structure of intermediate clustered states can be different [Fig. 10(d)]. We have also observed nonlocal synchronization [48,49], where an oscillator or a cluster of oscillators is synchronized not to a nearest oscillator or clusters of oscillators, but to a next-to-the-nearest-neighbor oscillator or cluster.

Two opposite effects are observed in the study of the influence of the noncoherence on the global synchronization in the chain. As in the case of two-element systems, a rather small increase of noncoherence of rotations practically does not change the size of the global synchronization region. But with a further increase of noncoherence even in the case of

the absence of coupling, some neighboring elements can have the same rotation numbers, i.e., they belong to one interval of equal rotation numbers (Fig. 1). Thus clusters of synchronization can exist without coupling. If the difference between rotation numbers of elements is small enough, then the occurrence of global synchronization happens for smaller coupling than in the case of weak noncoherence. There the common rotation number coincides with the rotation number of the elements in the largest cluster. Usually this situation is observed for intermediate values of c. For strong noncoherence the rotation number difference can be very large. Then in spite of the existence of synchronous clusters in an uncoupled chain, global synchronization can be observed only for stronger coupling (Fig. 11). Moreover, the transition to global synchronization in a chain of coupled regular CMs is rather complex in dependence on c (Fig. 11) that is in accordance with the two element case (Fig. 6).

C. Chaotic phase synchronization

Phase synchronization in ensembles of locally coupled chaotic elements was first studied in chains of weakly diffusively coupled chaotic Rössler oscillators [7]. Many phenomena already observed in a population of periodic oscillators were found there too, especially to mention the existence of several clusters of mutually synchronized elements and global synchronization. The collective behavior in a chain of coupled chaotic ($c<0$) CMs (7) exhibits similar properties. We have explored such a chain with linear and random individual frequency distributions. As in the case of regular noncoherent rotations for linearly distributed frequencies, both soft and hard transitions to global synchronization are observed. But in the case of randomly distributed frequencies, only a hard transition is possible. For a linear distribution of the individual frequencies the rich spatiotemporal dynamics of the noncluster (smooth distribution of rotation numbers) [Fig. 12(a)] and cluster synchronization structures [Fig. 12(b)] is illustrated in Fig. 13. In all plots the darker regions mark higher values of the presented variables. The two left panels show the quantity $\sin(x_n^k)$, so that the white stripes correspond to the phase $\approx 3\pi/2$ and the black stripes to the phase $\approx \pi/2$. The right panel shows the quantity

$$s_n = \sin^2\left(\frac{x_{n+1}^k - x_n^k}{2}\right), \tag{23}$$

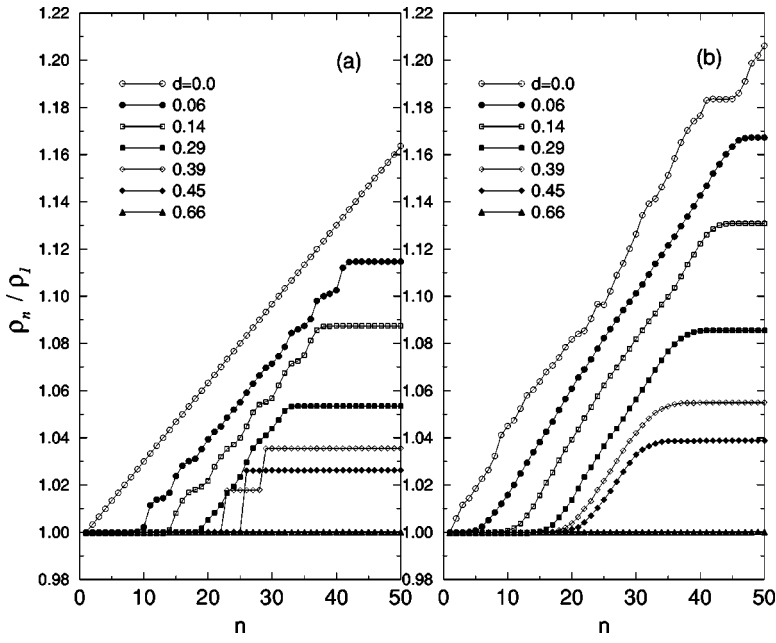which characterizes the instantaneous phase difference be-

FIG. 12. Hard (a) and soft (b) transitions to global chaotic phase synchronization. Relative rotation numbers ρ_n/ρ_1 for different coupling coefficients d for linear distribution of individual frequencies for $b_1=0.6$, frequency mismatch $\Delta b=0.002$, $c=-0.002$ (a) and $c=-0.4$ (b).

tween neighboring oscillators. We have then that $s_n=0$ if the phases are equal and $s_n=1$ if they differ by π. The spatiotemporal behavior of the boundaries between clusters corresponds to the positions where phase slips or defects occur.

These defects are clearly seen as maxima (black regions) of s_n. They can follow regularly in time at certain positions on the chain; this case corresponds to the existence of strong jumps between clusters [Fig. 13(c)]. If cluster structures do
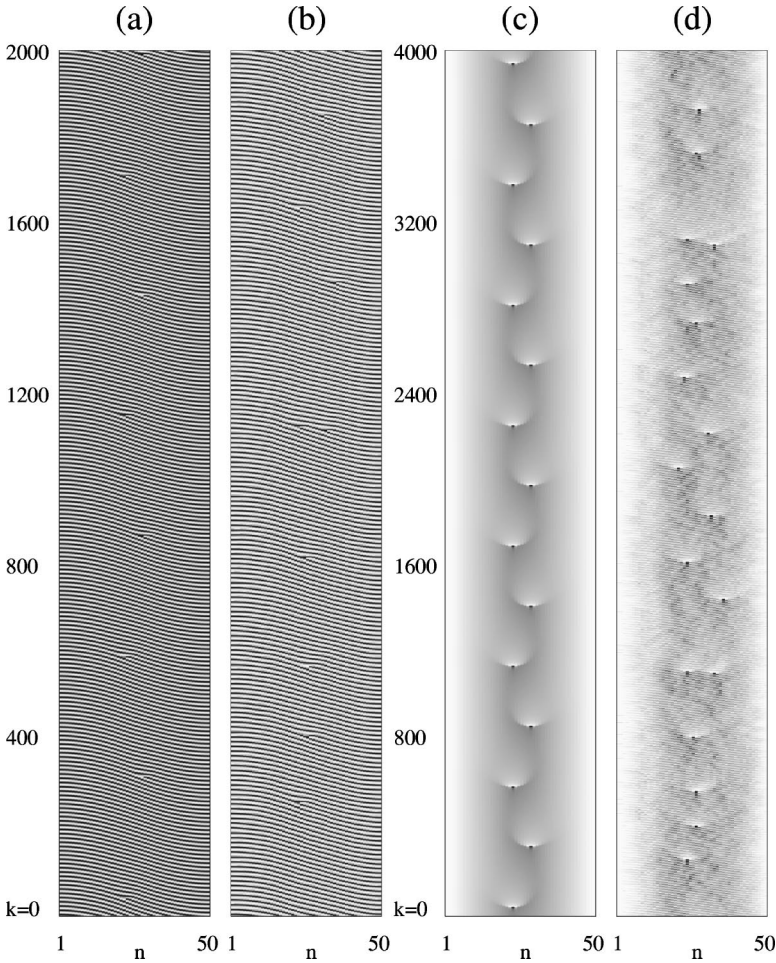

FIG. 13. Space-time plots of evolution of (a),(b) $\sin(x_n^k)$ and s_n [Eq. (23)] (c),(d) by hard (a),(c) and soft (b),(d) transitions to global chaotic phase synchronization for a linear distribution of individual frequencies. The parameters are $N=50$, $b_1=0.6$, frequency mismatch $\Delta b=0.002$, coupling $d=0.39$ and $c=-0.002$ (a),(c) and $c=-0.4$ (b),(d).

not exist or the borders between clusters are smooth, then defects appear irregularly in both space and time [Fig. 13(d)].

We have explored synchronization properties in a chain of 50 chaotic CMs with a linear distribution of individual frequencies b_n [Eq. (15)] for $b_1 = 0.6$, different values of frequency mismatch Δb and different values of c. For all performed simulations the following has been observed: With an increase of the parameter $-c$ the critical value of coupling d^+ that corresponds to the transition to global synchronization first slightly increases and then can decrease and increase again, and finally increases. After some critical value $-c^*$ a synchronization is impossible.

VI. CONCLUSIONS

We have observed a rich variety of phenomena in the formation of regular and chaotic phase synchronization in systems of coupled nonidentical circle maps. Two-element systems and chains of coupled elements have been examined. The main attention has been focused on the study of the influence of the power of the coherence of phase evolutions on the synchronization processes. In order to characterize the phase evolution, we have analyzed three parameters: (i) the rotation number ρ, (ii) the variance D of the phase evolution, and (iii) the parameter γ that defines the relative duration of the intervals of phase increase and phase decrease. We have shown that D, γ, and $\Delta\rho$ are crucial for the synchronization of chaotic CMs, whereas in the case of regular CMs only D and $\Delta\rho$ are important. It has been demonstrated that with an increase of the coherence parameter in the regular and chaotic regime, regions of main (1:1) synchronization are usually decreased.

We have found a chaotic synchronization: In systems of coupled nonidentical circle maps a phase entrainment occurs not through bifurcations, but through interior crises of a hyperchaotic set.

In the case of chains of coupled CMs, typical features of the onset and existence of global (all-to-all) and cluster (partial) synchronization have been explored. We have found two scenarios of transition to global synchronization. First, a gradual adjustment of the rotation numbers is observed, while second, the transition occurs through the appearance of synchronized clusters.

Our study supports the idea that phase synchronization is a general phenomenon of coupled chaotic systems that depends on phase-coherent properties of motions.

These findings in chains of coupled maps should be a subject of further experimental studies, especially to mention are the study of soft and hard transitions in chains of coupled chemical oscillators [50] or in coupled lasers [51] and the study to check whether there are also transitions to phase synchronization via interior crises.

Our result that synchronization can be destroyed through increasing coupling strength is of special importance for the design of DPLL in order to realize stable synchronization in engineering applications.

[1] A.S. Pikovsky, M.G. Rosenblum, and J. Kurths, *Synchronization—A Universal Concept in Nonlinear Sciences*, (Cambridge University Press, Cambridge, 2001).

[2] Int. J. Bifurcation Chaos Appl. Sci. Eng., **10** (2000).

[3] E. Stone, Phys. Lett. A **163**, 47 (1992).

[4] A.S. Pikovsky, M.G. Rosenblum, G.V. Osipov, and J. Kurths, Physica D **104**, 219 (1997).

[5] M.G. Rosenblum, A.S. Pikovsky, and J. Kurths, Phys. Rev. Lett. **76**, 1804 (1996).

[6] A.S. Pikovsky, M.G. Rosenblum, and J. Kurths, Europhys. Lett. **34**, 165 (1996).

[7] G.V. Osipov, A.S. Pikovsky, M.G. Rosenblum, and J. Kurths, Phys. Rev. E **55**, 2353 (1997).

[8] R.C. Elson *et al.*, Phys. Rev. Lett. **81**, 5692 (1998).

[9] V. Makarenko and R. Llinas, Proc. Natl. Acad. Sci. U.S.A. **95**, 15 474 (1998).

[10] B. Blasius, A. Huppert, and L. Stone, Nature (London) **399**, 354 (1999).

[11] C. Schäfer, M.G. Rosenblum, J. Kurths, and H.H. Abel, Nature (London) **392**, 239 (1998).

[12] P. Tass *et al.*, Phys. Rev. Lett. **81**, 3291 (1998).

[13] F. Mormann, K. Lehnertz, P. David, and Ch.E. Elger, Physica D **144**, 358 (2000).

[14] K. Kaneko, Physica D **75**, 55 (1994); **77**, 456 (1994); **86**, 158 (1995).

[15] B. Hu and Z. Liu, Phys. Rev. E **62**, 2114 (2000).

[16] F.S. de San Roman, S. Boccaletti, D. Maza, and H. Mancini, Phys. Rev. Lett. **81**, 3639 (1998).

[17] G.S. Gil and S.C. Gupta, IEEE Trans. Commun. **20**, 454 (1972).

[18] M. de Sousa Vieira, A.J. Lichtenberg, and M.A. Lieberman, Phys. Rev. A **46**, R7359 (1992).

[19] M. de Sousa Vieira, A.J. Lichtenberg, and M.A. Lieberman, Int. J. Bifurcation Chaos Appl. Sci. Eng. **1**, 691 (1994).

[20] G. Goldztein and S.H. Strogatz, Int. J. Bifurcation Chaos Appl. Sci. Eng. **5**, 983 (1995).

[21] V.S. Afraimovich, V.I. Nekorkin, G.V. Osipov, and V.D. Shalfeev, *Stability, Structures and Chaos in Nonlinear Synchronization Networks* (World Scientific, Singapore, 1995).

[22] N.F. Rul'kov and A.R. Volkovskii, Phys. Lett. A **173**, 332 (1993); A.R. Volkovskii, IEEE Trans. Circuits Syst. **44**, 913 (1997).

[23] Y. Kuramoto, Physica D **50**, 15 (1991); G.B. Ermentrout and N. Kopell, J. Math. Biol. **29**, 571 (1991); A. Treves, Network **4**, 259 (1993); M. Usher, H.G. Schuster, and E. Niebur, Neural

Comput. **5**, 570 (1993); M. Tsodyks, I. Mitkov, and H. Sompolinsky, Phys. Rev. Lett. **71**, 1280 (1995); T.L. Carroll, Biol. Cybern. **73**, 553 (1995); C.J. Perez Vicente, A. Arenas, and L.L. Bonilla, J. Phys. A **29**, L9 (1996); A. DiazGuilera, C.J. Perez, and A. Arenas, Phys. Rev. E **57**, 3820 (1998); T.D. Frank, A. Daffertshofer, C.E. Peper, P.J. Beek, and H. Haken Physica D **144**, 62 (2000).

[24] V. Torre, J. Theor. Biol. **61**, 55 (1976); J. Jalife, J. Physiol. (London) **356**, 221 (1984); D.C. Michaels, E.P. Matyas, and J. Jalife, Circ. Res. **61**, 704 (1987).

[25] T.L. Carroll, J. Heagy, and L.M. Pecora, Phys. Lett. A **186**, 225 (1994).

[26] A.T. Winfree, J. Theor. Biol. **16**, 15 (1967); G.B. Ermentrout, J. Math. Biol. **23**, 55 (1985); S.H. Strogatz and I. Stewart, Sci. Am. **269**(6), 102 (1993).

[27] A.T. Winfree, *The Geometry of Biological Time* (Springer-Verlag, New York, 1980); Y. Kuramoto, *Chemical Oscillations, Waves and Turbulence* (Springer, New York, 1984).

[28] P. Hadley, M.R. Beasley, and K. Wiesenfeld, Phys. Rev. B **38**, 8712 (1988); K. K. Likharev, *Dynamics of Josephson Junctions and Circuits* (Gordon and Breach, Philadelphia, 1991); S. Watanabe and S.H. Strogatz, Physica D **74**, 197 (1994); S. Watanabe, H.S.J. van der Zant, S.H. Strogatz, and T.P. Orlando, *ibid.* **97**, 429 (1996); K. Wiesenfeld, P. Colet, and S.H. Strogatz, Phys. Rev. Lett. **76**, 404 (1996); K. Wiesenfeld, P. Colet, and S.H. Strogatz, Phys. Rev. E **57**, 1563 (1998).

[29] H.G. Winful and S.S. Wang, Appl. Phys. Lett. **53**, 1894 (1988); M. Silber, L. Fabiny, and K. Wiesenfeld, J. Opt. Soc. Am. B **10**, 1121 (1993); L. Fabiny, P. Colet, R. Roy, and D. Lenstra, Phys. Rev. A **47**, 4287 (1993); P.M. Alsing, A. Gavrielides, V. Kovanis, R. Roy, and K.S. Thornburg, Phys. Rev. E **56**, 6302 (1997).

[30] A. Katok and B. Hasselblatt, *Introduction to the Modern Theory of Dynamical Systems* (Cambridge University Press, Cambridge, 1995).

[31] H.G. Schuster, *Deterministic Chaos, an Introduction* (VCH-Verlag, Weinheim, 1988); K.T. Alligood, T.D. Sauer, and J.A. Yorke, *Chaos: An Introduction to Dynamical Systems* (Springer, New York, 1992); E. Ott, *Chaos in Dynamical Systems* (Cambridge University Press, Cambridge, 1992); J. Argyris, G. Faust, and M. Haase, *An Exploration of Chaos* (North-Holland, Amsterdam, 1994).

[32] W.C. Lindsey, *Synchronization Systems in Communication and Control* (Prentice-Hall, Englewood Cliffs, NJ, 1972).

[33] I.P. Keener, Trans. Am. Math. Soc. **26**(2), 589 (1980).

[34] R. Klages and J.R. Dorfman, Phys. Rev. Lett. **74**, 387 (1995).

[35] M.I. Malkin, *Differential Equations Theory Methods* (Gorky State University, Gorky, 1986), p. 122 (in Russian).

[36] S.H. Strogatz and R.E. Mirollo, Physica D **31**, 143 (1988); H. Sakaguchi, S. Shinomoto, and Y. Kuramoto, Prog. Theor. Phys. **77**, 1005 (1987); A.H. Cohen, P.J. Holmes, and R.H. Rand, J. Math. Biol. **13**, 345 (1982); G.B. Ermentrout, *ibid.* **23**, 55 (1985); G.B. Ermentrout and N. Kopell, SIAM (Soc. Ind. Appl. Math.) J. Math. Anal. **15**, 215 (1984); I.N. Klibanova, A.N. Malakhov, and A.A. Mal'tsev, Radiophys. Quantum Electron. **14**, 173 (1971); N. Kopell and G.B. Ermentrout, Commun. Pure Appl. Math. **39**, 623 (1986); L. Ren and G.B. Ermentrout, SIAM (Soc. Ind. Appl. Math.) J. Math. Anal. **29**, 208 (1998); Z. Zheng, G. Hu, and B. Hu, Phys. Rev. Lett. **81**, 5318 (1998).

[37] L.M. Pecora, Phys. Rev. E **58**, 347 (1998).

[38] J.F. Heagy, T.L. Carroll, and L.M. Pecora, Phys. Rev. Lett. **73**, 3528 (1995); J.F. Heagy, T.L. Carroll, and L.M. Pecora, Phys. Rev. E **52**, R1253 (1995); J.F. Heagy, L.M. Pecora, and T.L. Carroll, Phys. Rev. Lett. **74**, 4185 (1995).

[39] S. Watanabe *et al.*, Physica D **97**, 429 (1996).

[40] D. Rand, S. Ostlund, J. Sethna, and E.D. Siggia, Phys. Rev. Lett. **49**, 132 (1982).

[41] S.J. Shenker, Physica D **5**, 405 (1982).

[42] E. Ott, *Chaos in Dynamical Systems* (Cambridge University Press, Cambridge, 1992).

[43] M.A. Zaks, E.-H. Park, M.G. Rosenblum, and J. Kurths, Phys. Rev. Lett. **82**, 4228 (1999).

[44] It is interesting to note that as one can see from the conditions of existence and stability of fixed point in the *sinus* circle map (10), 1:1 synchronization can occur for CMs at $c = 0$ with contrary rotating phases, i.e., for example at $b_1 < 0 < b_2$.

[45] A. Pikovsky, G. Osipov, M. Rosenblum, M. Zaks, and J. Kurths, Phys. Rev. Lett. **79**, 47 (1997).

[46] G.B. Ermentrout and N. Kopell, SIAM (Soc. Ind. Appl. Math.) J. Math. Anal. **15**, 215 (1984).

[47] G.V. Osipov and M.M. Sushchik, Phys. Rev. E **58**, 7198 (1998).

[48] G.V. Osipov and M.M. Sushchik, Phys. Lett. A **201**, 205 (1995).

[49] M. Zhan, Z.G. Zheng, G. Hu, and X.H. Peng, Phys. Rev. E **62**, 3552 (2000).

[50] W. Wang, I.Z. Kiss, and J.L. Hudson, Phys. Rev. Lett. **86**, 4954 (2001).

[51] D. DeShazer *et al.*, Phys. Rev. Lett. **87**, 044101 (2001); E. Allaria *et al.*, *ibid.* **86**, 791 (2001).